ROMANIAN JOURNAL OF INFORMATION SCIENCE AND TECHNOLOGY
Volume **18**, Number 4, 2015, 388–407

Low-Voltage Controlled Floating Buck Converter with Imbalanced Stacked MOSFETs Switch (ISMS) for High LED Driving Capability

Anca Gabriela PURDILA[1,2], Gheorghe PRISTAVU[2], Vlad ANGHEL[1], Gheorghe BREZEANU[2], Emilian CEUCA[3]

[1]ON Semiconductor, Bucharest, Romania (Signal and Interface Group)
[2]"Politehnica" University of Bucharest, Romania (Faculty of Electrical Engineering)
[3]"1 Decembrie 1918" University of Alba Iulia, Romania

E-mail: anca.vasilica@onsemi.com, gheorghe.pristavu@dcae.pub.ro, vlad.anghel@onsemi.com, gheorghe.brezeanu@dce.pub.ro, eceuca_2008@yahoo.ro

Abstract. This paper presents a cost effective technique for extending LED driving capability of floating buck converters, using an imbalanced stacked MOSFETs switch (ISMS). The ISMS is comprised of a low-voltage transistor and a power MOSFET, biased at a constant voltage, and can be driven by low output capability control blocks. Unlike prior-art, the proposed ISMS does not rely on synchronous switching and identical devices. The overall turn ON/OFF times impact on the converter's switching frequency is investigated. The proposed technique is validated by implementation in floating buck converters with two high performing control circuits. Hence, a critical conduction mode control block and a variable OFF time controller, fabricated in 40 V and 5 V CMOS technologies, respectively, are used for driving the converter. Measurements are performed for a wide range of LED strings (6-48) and up to 250 V input voltage. Efficiency results reveal a peak value of 97% and switching frequencies between 25 KHz and 170 KHz. Converters with ISMS are experimentally proven to drive up to eight times more LEDs than their regular versions, with higher efficiencies.

Key words: stacked MOSFETs; floating buck LED driver; low-voltage control; critical conduction control; variable OFF time control.

1. Introduction

LED backlit LCD TVs have recently seen a steep rise in demand due to high luminous efficacy, long lifetime and dimming capabilities [1]. This trend paved the way for a plethora of LED driving methods, including switch-mode power supplies. Depending on the type of backlighting (direct, segment or edge lit), the number of series connected LEDs can vary up to 50 devices, while input voltages required to drive them can reach 250 V [2]. As the display sizes increase, so will these numbers. Thus, the need for high-voltage compliant ICs has put a roadblock in reducing the cost gap between LED TVs and their cold cathode fluorescent lamps (CCFL) counterparts. As a result, solutions for interfacing high and low-voltage supply rails are sought.

Floating buck converters for LED driving in LCD TV applications employ a typical architecture [3]–[19]. The switch-mode operation of these circuits imposes certain performance requirements on the switching transistor. When in the OFF state, its drain-source voltage is roughly equal to the input voltage. As such, when driving large numbers of LEDs, a switching transistor with high drain-source voltage capabilities is necessary. Controllers with an integrated switch must therefore be fabricated in expensive high-voltage technologies. Even if the switching transistor is external, the controller should still offer strong driving capabilities, which also takes its toll on technological cost.

This paper proposes a technique to extend the number of driven LEDs in floating buck converters, using an imbalanced stacked MOSFETs switch (ISMS). This stack has a high voltage blocking capability and can also be driven by a low voltage, cost effective control block. Moreover, the ISMS technique can be adapted to control blocks with both integrated and external switches. The proposed solution's effectiveness is proven for floating buck converters using two different control architectures [15], [19].

The paper is organized as follows. Section 2 describes the proposed technique for extending the number of series connected LEDs driven by a floating buck converter. Section 3 analyzes the switching sequence of the stacked MOSFETs structure. In Section 4, a brief overview of the existing control methods is presented, emphasizing some of the most important advantages for each. The next section, Section 5, is focused on integrating the proposed ISMS in floating buck converters with two high performing control methods. Experimental results, reported in Section 6, are obtained by measurements on the floating buck converter for a wide range of input voltages and number of LEDs in the string. Conclusions are finally drawn in Section 7.

2. Floating Buck Converter With SMS

Floating buck converters (also known as reverse or inverted) are often used in LED driving applications and employ a standard architecture [3]–[19], depicted in Fig. 1a. The number of driven LEDs is limited by the input voltage.

Standard applications use a single nMOS transistor as SW (Fig. 1a), either external or integrated with its control block. The maximum input voltage value (and, implicitly, maximum number of LEDs) is limited by the drain-source voltage capa-

bilities ($V_{DS,max}$) of this device. Applications that drive a high number of series connected LEDs must therefore utilize a high voltage capability switch. This power device requires a substantially increased driving capability. Switching speed, breakdown voltage and ON resistance are the main concerns when selecting our power switch.

Stacking transistors is a well documented and preferred technique of achieving high voltage tolerant switches [20], [21], [22]. Having multiple series connected transistors successfully distributes workload [21], so that each device withstands a safe power dropout. As stated in [23], [24], there are three basic stacked transistor topologies: stacked MOSFETs, stacked IGBTs and emitter-switched bipolar transistor (ESBT). Power MOSFET devices require low driving power and have high switching speeds, but suffer from high ON resistance. While IGBTs offer superior conduction properties, their switching times are significantly higher. Both series-connection topologies are made up of identical devices and require additional circuitry to ensure safe synchronous switching. The best overall performance is achieved by a hybrid topology, the ESBT [24], obtained by stacking a high-voltage bipolar transistor on a low-voltage MOSFET. This is a high cost architecture which also requires a significant driving capability for the BJT. Moreover, technological cost of control blocks capable of delivering high driving capabilities, especially when integrated with the switch, is considerably greater than a generic 5V controller.

In this paper, an imbalanced stacked MOSFETs switch (ISMS) is derived from the basic ESBT topology in order to obtain a high voltage blocking structure, which has high switching speed and is cost-effective (does not require high gate driving capabilities). Unlike prior-art [20], [21], [22], the proposed ISMS is not reliant on synchronous switching and identical devices. Instead of gate capacitors charged by a resistive divider, our structure uses an external voltage reference, eliminating the biasing resistors' losses [20], [21].

The enhanced architecture for the floating buck converter with the proposed imbalanced stacked MOSFETs switch is depicted in Fig. 1b.

The ISMS includes SW_1 and SW_2. SW_1 (Fig. 1b) is a low voltage transistor with low gate capacitance, which can achieve fast switching using a low-voltage control block [18], [19]. Under these circumstances, SW_2 (Fig. 1b) should be a power MOSFET, whose high drain-source voltage capability allows the converter to drive a significantly increased number of LEDs. This power device is biased at a constant gate voltage (V_{GG} – Fig. 1b). The Schottky diode DS_L is included in order to limit the maximum drain-source voltage drop on SW_1 to V_{GG}. This technique can also be applied when SW_1 is integrated with the control block.

The proposed switch has significantly lower driving requirements than both ESBT and synchronous-switched stacked MOSFETs, at the cost of increased ON resistance.

The ISMS is directly driven by the control block through V_{DRV}. The current through the inductor varies between two thresholds (I_{VALLEY} and I_{PEAK}), determining the value for the average LED current (I_{AVG}). The duty-cycle and switching frequency are adjusted in order to maintain the desired value for I_{AVG}. When designing the application, it is necessary that the converter switching period be much higher than the SMS's turn-ON and turn-OFF times so as not to affect the accuracy of the

average current. Because the proposed ISMS does not rely on synchronous switching, its transition time is slightly higher than state-of-the-art stacked topologies. The following section analyzes the turn-ON and turn-OFF sequences for the ISMS.

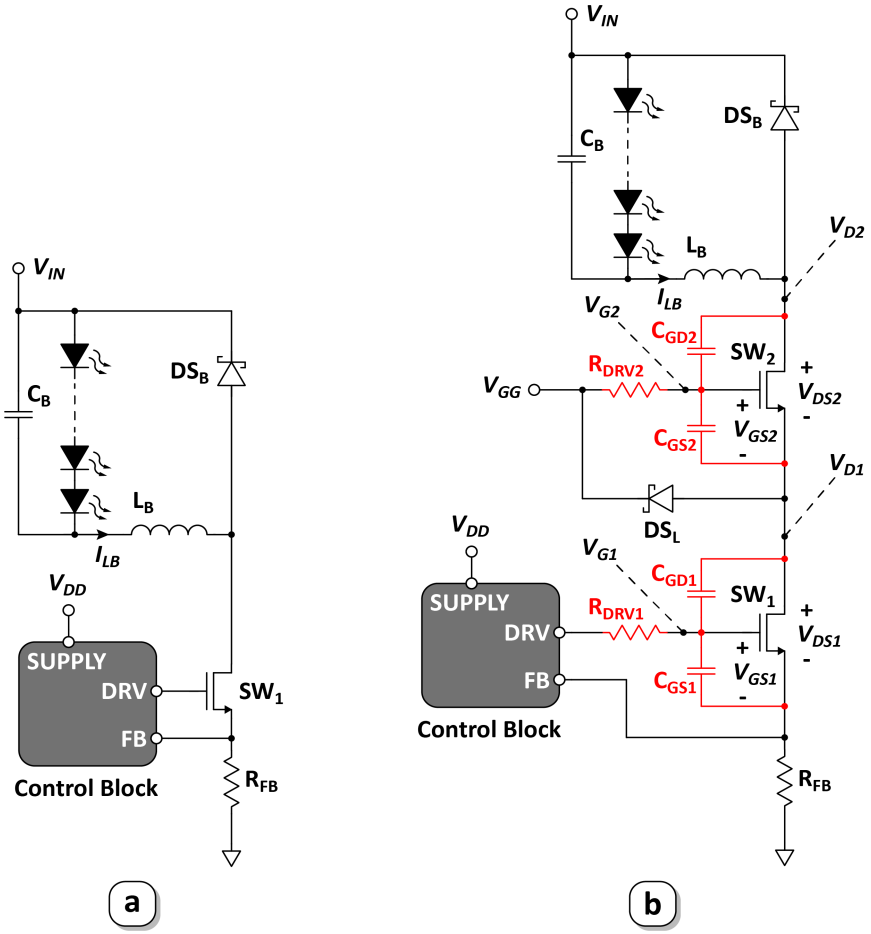

Fig. 1. Floating buck converter – standard architecture (a) and enhanced architecture (with imbalanced stacked MOSFETs switch – ISMS) (b).

3. ISMS Switching Sequence

The detailed switching transitions are illustrated in Fig. 2. The turn-ON sequence (a) is initiated when the control block applies a ramp from 0 to V_{DD} at the DRV output. After the gate-source voltage of SW_1 reaches its threshold value (V_{T1}), its drain-source voltage starts decreasing because there is no current path allowed by

SW_2. V_{GS2} increases accordingly until the threshold voltage (V_{T2}) is exceeded. SW_2 enters conduction mode and the ISMS current (I_{ISMS}– Fig. 2a) starts overtaking the inductor current. Finally, the drain-source voltages of SW_1 and SW_2 sequentially drop (first for SW_2, then for SW_1), marking the end of the turn-ON sequence.

It can be seen that, for the turn-ON sequence (Fig. 2a), the total amount of time required is:

$$t_{T-ON} = t_{1a} + t_{2a} + t_{3a}. \tag{1}$$

This time interval depends on the lumped gate resistances of the two MOSFET switches and their intrinsic capacitances (C_{gs} and C_{gd}, see Fig. 1b) [25]. The first interval (t_{1a} – Fig. 2a) represents the time needed for the gate-source of SW_1 to charge exponentially to its threshold voltage (V_{T1} – Fig. 2a), given by [25]:

$$t_{1a} = \tau_{1-ON} \ln\left(\frac{V_{DD}}{V_{DD} - V_{T1}}\right), \tag{2}$$

where $\tau_{1-ON} = R_{drv1-ON} \cdot (C_{gs1} + C_{gd1})$. $R_{drv1-ON}$ represents the SW_1 lumped gate resistance during the ON transition [25].

Interval t_{2a} (t'_{2a} and t''_{2a} – Fig. 2a) represents the total charge time of V_{GS2} voltage from 0 V to $0.9 \cdot V_{GG}$. Its expression is:

$$t_{2a} = \tau_{2-ON} \ln\left(\frac{V_{GG}}{V_{GG} - 0.9 \cdot V_{GG}}\right) = \tau_{2-ON} \ln(10), \tag{3}$$

where $\tau_{2-ON} = R_{drv2-ON} \cdot (C_{gs2} + C_{gd2})$. The t_{3a} time is the Miller plateau interval (Fig. 2a) and corresponds to V_{DS2} decrease from approximately V_{IN} to 0 V:

$$t_{3a} = V_{IN} \cdot \frac{R_{drv2-ON} \cdot C_{gd2}}{V_{GG} - V_{GS2}}. \tag{4}$$

The turn-OFF sequence (Fig. 2b) begins when the control block applies a slope from V_{DD} to 0 at the DRV output. The gate-source voltage of SW_1 drops towards the minimum value required to support the full inductor current ($V_{T1} + V_{ov1}$ – Fig. 2b). V_{DS1} starts to increase, determining V_{GS2} to decrease until it also reaches the limit required to support the inductor current($V_{T2} + V_{ov2}$ – Fig. 2b). V_{DS2} swings close to V_{IN} until the DS_B freewheeling diode becomes directly biased. This transition is followed by the decrease of the ISMS current to zero due to DS_B progressively overtaking the inductor current. Finally, the gate-source voltage of SW_2 falls, marking the end of the turn-OFF sequence.

Similarly to t_{T-ON}, the turn-OFF sequence (Fig. 2b) consists of a sum of three terms representing V_{GS1} and V_{GS2} total discharge times (t_{1b} and t_{2b}, respectively), coupled with V_{DS2} swing time (t_{3b}):

$$t_{T-OFF} = t_{1b} + t_{2b} + t_{3b} \tag{5}$$

$$t_{1b} = \tau_{1-OFF} \ln\left(\frac{V_{DD}}{V_{DD} - V_{T1} - V_{ov1}}\right) \tag{6}$$

$$t_{2b} = \tau_{2-OFF} \ln(10) \tag{7}$$

$$t_{3b} = V_{IN} \cdot \frac{R_{drv2-OFF} \cdot C_{gd2}}{V_{T2} + V_{ov2}} \tag{8}$$

where $\tau_{1,OFF} = R_{drv1-OFF} \cdot (C_{gs1} + C_{gd1})$, $\tau_{2,OFF} = R_{drv2-OFF} \cdot (C_{gs2} + C_{gd2}) \cdot$ $\cdot R_{drv1,2-OFF}$ represent the lumped gate resistances for each transistor during the OFF transition [25].

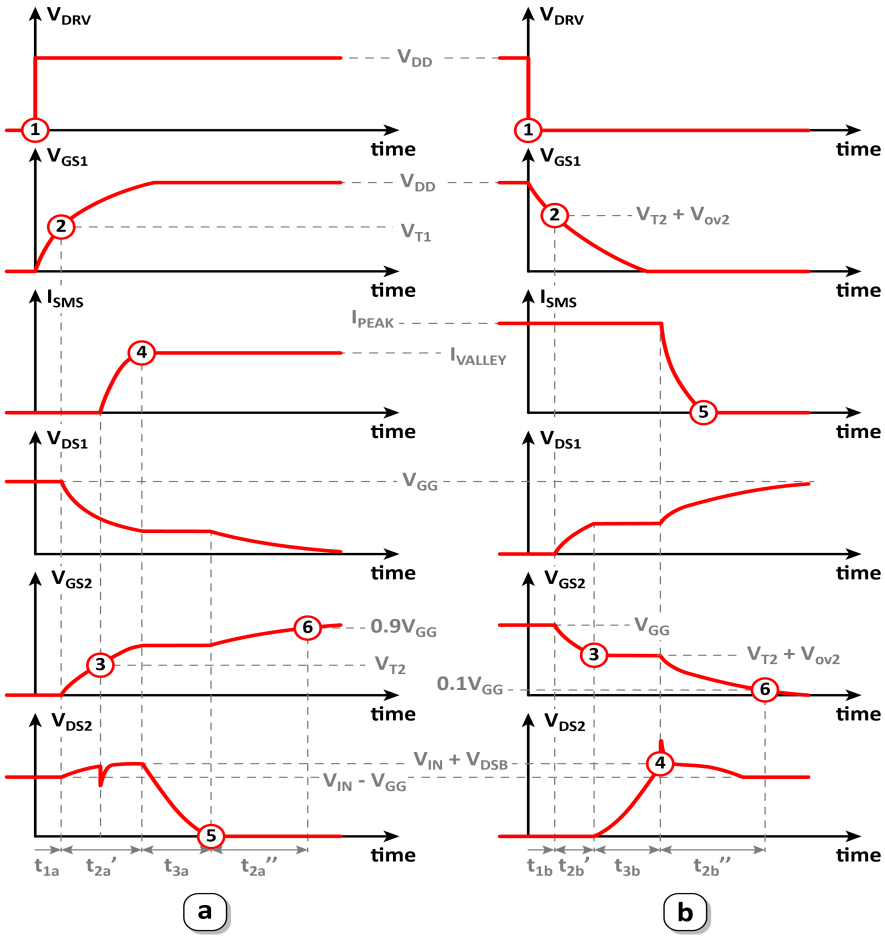

Fig. 2. Detailed turn-ON (a) and turn-OFF (b) times for the proposed stacked MOSFETs switch.

Overall, the turn ON and OFF times of the ISMS are determined primarily by $t_{2a,b}$ and $t_{3a,b}$. This is because the internal capacitances of SW_2 are much greater than those of SW_1. Also, the V_{GG} voltage can greatly impact the total turn-ON/OFF durations. Its value should be high enough to minimize the switching sequence times, but also lower than the maximum drain-source voltage of SW_1. The effectiveness of

implementing the proposed ISMS into a floating buck converter also depends on its control block.

The following section reviews control methods in order to identify the most adequate solution for incorporating the ISMS.

4. Brief Overview Of Control Methods

The control block is used for driving the switch, setting a duty-cycle that ensures a desired, precise value for the current through the string of LEDs. It may have different architectures, which rely on either constant or variable switching frequency [26]. Each topology implies a series of advantages and drawbacks. Thus, selecting a control method is primarily conditioned by application specifications. Figure 3 summarizes the benefits of some of the most representative control techniques.

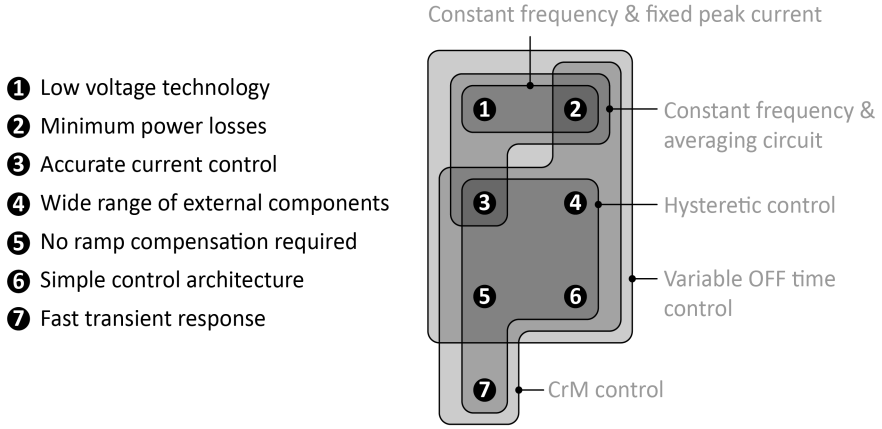

Fig. 3. Advantages of several representative control techniques for floating buck converters.

The constant frequency and fixed peak current control method offers advantages such as minimal power losses and cost effectiveness [5]–[9] (Fig. 3). In order to properly regulate the LED current, this topology uses the information provided by a grounded feedback resistor (R_{FB} – Fig. 1a) only during the ON time. Thus, the control block can be manufactured in a low-voltage technology, greatly alleviating fabrication cost. On the other hand, average LED current accuracy is low and strongly dependent on the external components' values (input voltage, number of LEDs, inductor).

The latest trend in constant frequency topologies is to employ an averaging circuit, substantially improving the current accuracy [10]–[13] (Fig. 3). Even so, the constant switching frequency operating mode still imposes harsh constraints on external component selection. Moreover, these control techniques are vulnerable to subharmonic oscillations and require ramp compensation [10]–[13], [27], [28]. The resulting circuit complexity increases, further limiting its general purpose capability.

The hysteretic control method exhibits complementary performances to its fixed frequency counterparts (Fig. 3). The inductor current varies between fixed thresholds regardless of the switching period [5], [6], [14]. As a result, the tolerable range for external components is much larger without affecting LED current accuracy. Moreover, the transient response to external parameter variations settles in a single switching cycle. However, current monitoring during the OFF time is required, which implies control block manufacturing in high voltage technologies, especially for driving large strings of LEDs. Also, because the sensing resistor is connected in series with the inductor, the power losses increase [6], [14].

The critical conduction mode (CrM) control method has the same operating principle (fixed thresholds for the inductor current) and advantages as the hysteretic technique (Fig. 3). The main difference is the zero value for the lower threshold. In this case, the feedback resistor is once again grounded, so the power losses are reduced [15]–[17].

Our previously introduced controller architecture, relying on variable OFF time [18] finds an advantageous compromise between fixed frequency, hysteretic and CrM topologies'characteristics, inheriting all benefits except fast transient response (Fig. 3).

The proposed LED string extension technique using ISMS can be used in floating buck converters with any of the above control methods. In order to get the best out of the application, a control technique with variable frequency is preferred. The next section is focused on integrating the proposed stacked MOSFETs switch in floating buck converters with CrM (V.1) and variable OFF time (V.2) control architectures, due to the high number of provided benefits (Fig. 3).

5. Proof Of Concept

5.1. Critical conduction mode (CrM) control

Figure 4a depicts the floating buck converter's standard architecture with a CrM control block. The latter monitors the current through the inductor and turns the switch (SW_1 – Fig. 4a) OFF and ON when its value reaches a maximum threshold and zero (by ZCD, a zero current detection circuit [29]), respectively.

In the basic topology (Fig. 4a), the control block architecture incorporates two comparators that detect both the maximum and zero thresholds for the inductor current [15]. The peak current detection is performed by monitoring the voltage drop on the R_{FB} resistor and comparing it with an internally generated voltage reference (V_{PEAK}). When V_{FB} exceeds V_{PEAK}, the switch is turned OFF. For the zero current detection, the C_2 comparator senses the forward voltage of the DS_B Schottky diode. When the current through the inductor reaches 0, all current paths are closed, and DS_B voltage becomes zero. V_{ZCD} becomes equal to V_{IN} and the C_2 comparator triggers zero current detection, turning SW_1 ON.

Depending on the voltage capabilities of the control block, the maximum V_{IN} value and, implicitly, the maximum number of driven LEDs are limited. In order to increase this number, the proposed ISMS has been incorporated by stacking a high

power switch (SW_2 – Fig. 4b) on SW_1. The supply voltage of the control circuit (V_{SUPPLY} – Fig. 4b) must be connected to an external power supply, because a high value for V_{IN} is required.

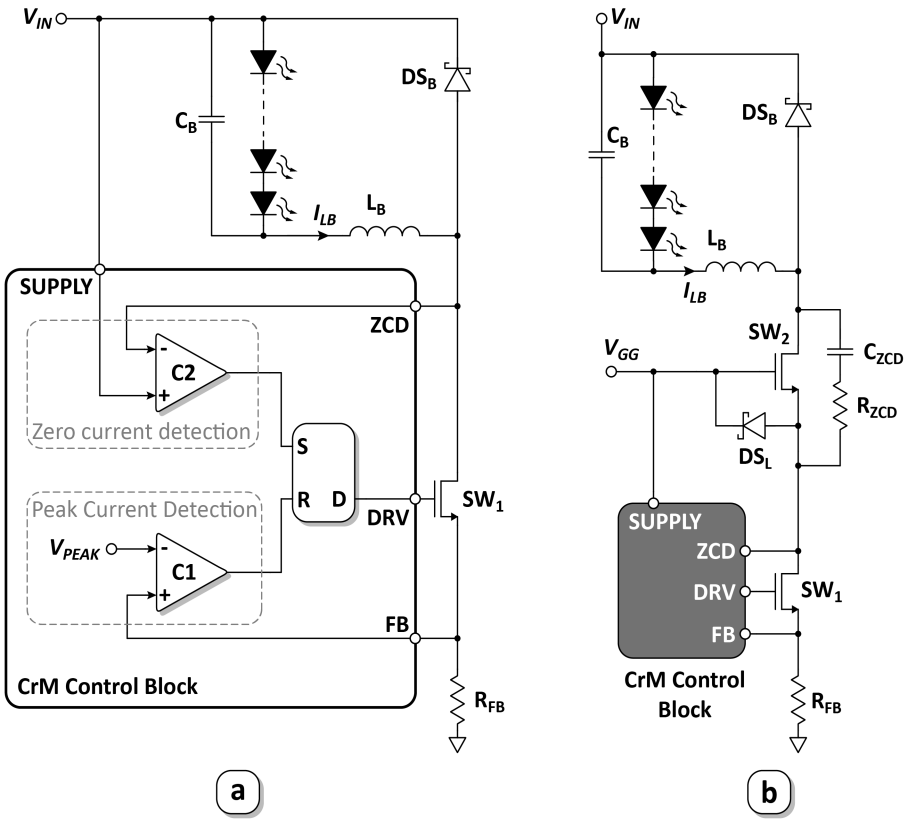

Fig. 4. Floating buck converter with CrM control block – standard (a) and enhanced architectures (b).

The addition of the stacked MOSFET (SW_2) requires an adjustment in the way zero current detection is performed. Hence, resistor R_{ZCD} and capacitor C_{ZCD} are also included. As can be seen in Fig. 4b, the voltage difference between the two inputs of the C2 comparator is now given by DS_L forward voltage. This diode is directly biased by the $R_{ZCD}-C_{ZCD}$ tank that overtakes a small amount of the inductor current when the ISMS is OFF. Now, the L_B current decreases until it reaches zero. At this point, DS_B and DS_L forward voltages become zero. This once again determines ZCD and SUPPLY pin potentials to be equal and the C_2 comparator detects zero inductor current, turning SW_1ON. The triggering conditions are time-wise nearly identical (for both architectures in Fig. 4), so the control circuit maintains its functionality also when driving larger strings of LEDs.

5.2. Variable OFF Time Control

The proposed ISMS was also incorporated in a floating buck converter with variable OFF time control block. Our previously introduced fixed peak current and variable OFF time controller (see Fig. 3) is used [19]. Figure 5 illustrates the converter's architecture both without (Fig. 5a) and with ISMS (Fig. 5b).

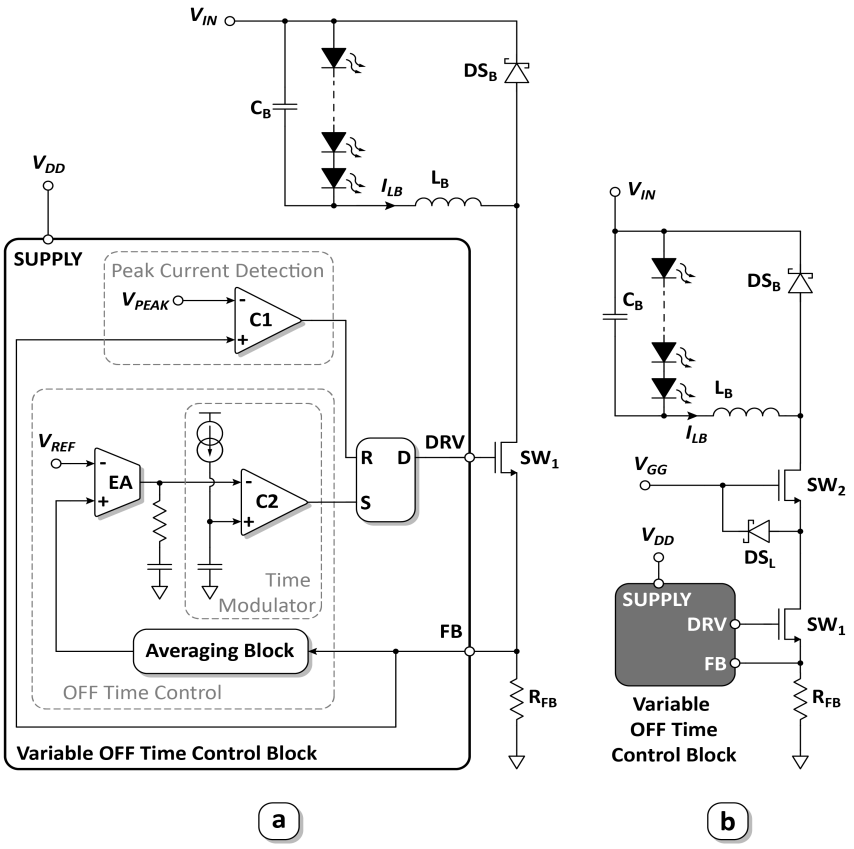

Fig. 5. Floating buck converter with variable OFF time control block – standard (a) and enhanced architecture (b).

The variable OFF time control block monitors the current through the inductor and turns the external switch (SW_1 – Fig. 5) OFF when its value reaches a predefined threshold. This action is performed in the same manner as for the CrM converter. During the ON time, the averaging block monitors the voltage drop on R_{FB} and outputs its mean value (V_{AVG}), which is then compared to the internal reference V_{REF} [18], [19]. Depending on the difference between V_{AVG} and V_{REF}, the time modulator block adjusts the OFF time in order to obtain a constant average current of V_{REF} / R_{FB} through the inductor [19].

The control block can be manufactured in a low-voltage, cost efficient technology, with modest driving capabilities. Therefore, it may command an external low power MOSFET as a switch (SW_1 – Fig. 5), with small input capacitance. On the other hand, the SW_1 low drain-source voltage capability allows the converter to drive only few LEDs.

In order to increase LED driving capability, a ISMS was incorporated (Fig. 5b). Hence, a high-power $SW_2$is once again stacked on the existing low-power MOSFET (SW_1). Unlike the CrM architecture (Fig. 4b), there is no need for additional components in order to ensure adequate operation of the control block, as there is only a low-side detection performed.

6. Experimental Results

In order to analyze the performances of the proposed technique, floating buck converter applications with ISMS were developed for both CrM and variable OFF time control architectures. Figure 6 shows the photograph of the experimental setups used for validating the proposed LED string extension technique.

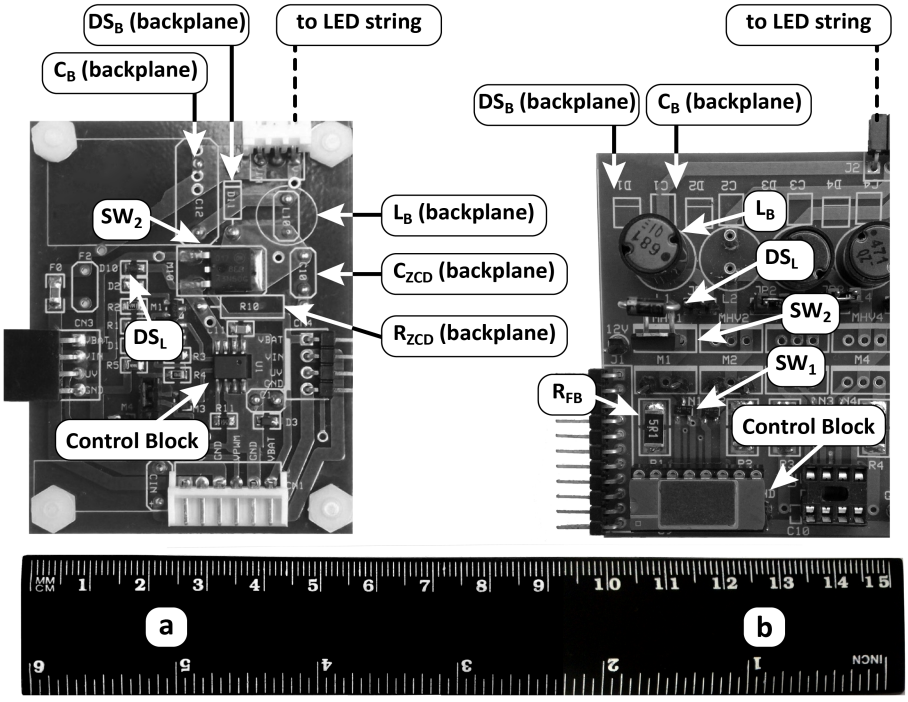

Fig. 6. Practical implementation of floating buck converters with ISMS using CrM (a) and variable OFF time (b) control blocks.

Initially, a commercially available CrM control block [16] was chosen for investigating the ISMS technique. For the basic topology, without stacked transistors, the input voltage is limited by the integrated switch (SW_1, Fig. 4a) to a maximum 40 V. As a result, the converter can drive up to 8 LEDs [16]. By incorporating the proposed ISMS (Fig. 4b) using the NDD05N50Z device, with 500 V maximum drain-source voltage capability [30] as SW_2, the LED limit is transcended. Note that a power supply as low as 12 V is enough to bias the control circuit and the gate of the power switch.

The designed values for C_{ZCD} and R_{ZCD} are 470 pF and 22 kΩ, respectively. These results were validated through the PSpice simulations illustrated in Fig. 7. Cursors A1 and A2 mark the zero voltage – current crossing for the DS_B and DS_L diodes, respectively. The 75 ns time difference can be considered negligible in respect to the 19.7 μs switching period. Moreover, the maximum C_{ZCD} current is 2.5 mA, much lower than the maximum inductor current of 500 mA.

The improved converter's functionality was experimentally validated for a wide range of numbers of LEDs (up to 48) and input voltages (up to 250 V). The measured efficiency is depicted in Fig. 8. Very high values, with a maximum of 97%, were obtained throughout the entire V_{IN} range. It is noted that, for each number of LEDs, the efficiency decreases inversely proportional to V_{IN}.

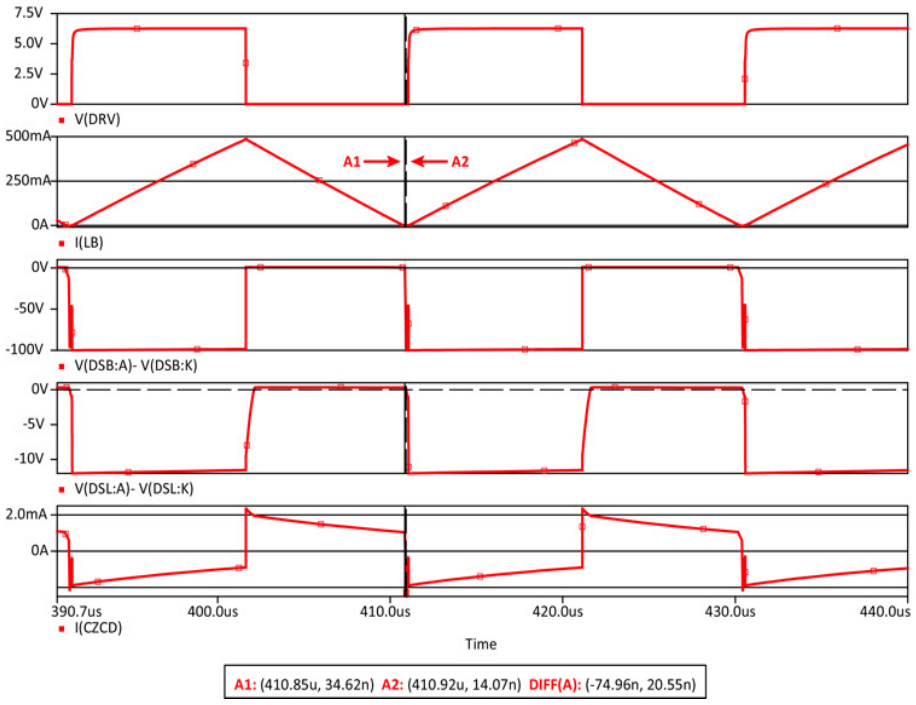

Fig. 7. Zero current detection for the ISMS CrM converter – simulation results for V_{IN} = 100 V, 15 LEDs, I_{AVG} = 250 mA and L_B = 1 mH.

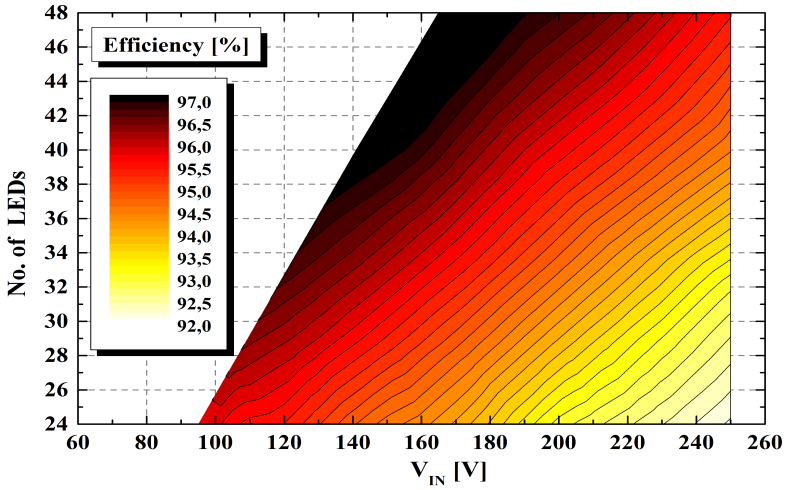

Fig. 8. Measured efficiency results for the ISMS CrM converter.

Figure 9 shows the measured switching frequency as a function of input voltage and number of LEDs. Operating frequencies varying from 25 to 115 kHz were recorded. It can be seen that, for a fixed number of LEDs, the switching frequency is directly proportional to the input voltage. Also, a complementary analysis of both plots from Figs. 8 and 9 emphasizes an efficiency increase in the lower switching frequency range. This is mainly due to the switching losses, which obviously occur more often at higher frequencies.

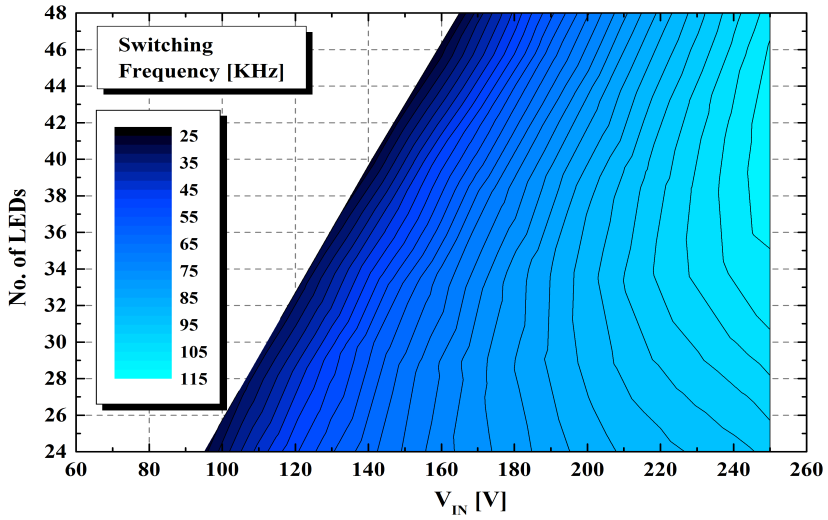

Fig. 9. Measured switching frequency results for the ISMS CrM converter.

The proposed ISMS technique was also implemented in a floating buck converter operating with the variable OFF time control circuit from Fig. 5a. The latter is manufactured in a low-cost, 0.5 µm CMOS technology, with a maximum allowed supply voltage of 5 V. Hence, in the basic topology, an external NTA4001N device was used as SW_1 due to its low gate capacitance [31]. However, its 20 V maximum drain–source voltage [31] determines a maximum input voltage of 20 V and, implicitly, up to 4 LEDs can be driven [19]. The ISMS topology was built with the same NDD05N50Z transistor as SW_2. Due to the proven versatility of the controller [19], proper LED driving is achieved for V_{GG} as low as 7 V.

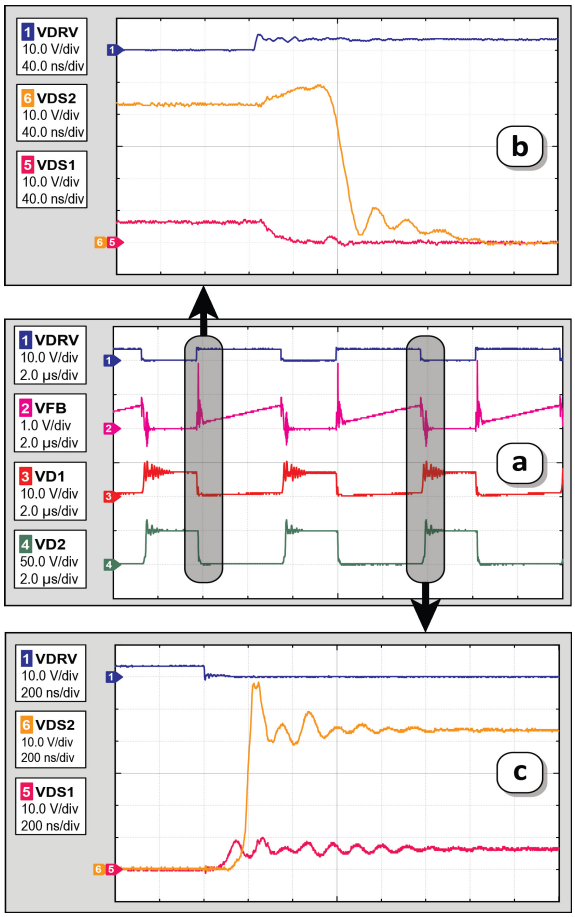

Fig. 10. Converter oscilloscope waveforms (a) with zoom on turn-ON (b) and turn-OFF (c) times – L_B = 680 µH, 10 LEDs, V_{IN} = 50 V and V_{GG} = 7 V.

The oscilloscope waveforms from Fig. 10 illustrate the ISMS converter operation for V_{IN} = 50 V, L_B = 680 µH, n = 10 LEDs, V_{DD} = 5 V and I_{AVG} = 100 mA. During the OFF state, V_{D1} is limited to roughly V_{DD}, ensuring the safe operation

of the low voltage switch (SW_1). The excess voltage up to V_{IN} is supported by the high voltage transistor (SW_2). Figures 10b and 10c emphasize turn-ON and turn-OFF sequences for the ISMS. Waveforms are consistent with the analytical study performed in Section 3 and depicted in Fig. 2. Measured values for turn-ON/OFF times are $t_{T-ON} = 120$ ns and $t_{T-OFF} = 350$ ns. These values are much lower than the converter switching period (*i.e.* 6 µs). The V_{DS2} waveforms confirm that the turn-ON and OFF times are determined mainly by SW_2's switching sequence.

Measurements were also performed on the variable OFF time converter with ISMS for V_{IN} up to 100 V, driving 100 mA through up to 30 LEDs. Figures 11 and 12 show the converter efficiency and switching frequency, respectively. The measurements were performed maintaining the same inductor ($L_B = 680$ µH).

Similar to the CrM converter, the efficiency decreases with input voltage. However, efficiencies of over 87% can be obtained for all cases. The most favorable scenario is when the input voltage value is very close to the voltage drop on the string of LEDs. A maximum efficiency of 93% was recorded (Fig. 11). Switching frequencies between 50 and 170 kHz were obtained for the entire voltage range (Fig. 12).

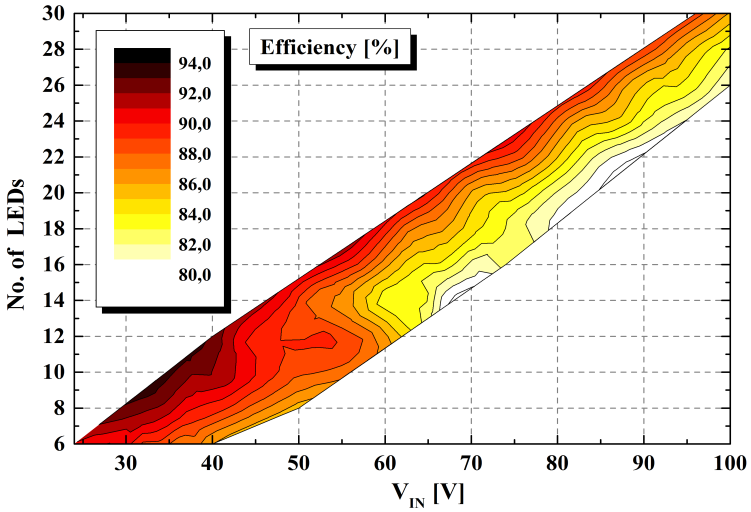

Fig. 11. Measured efficiency results for the ISMS variable OFF time converter.

Table 1 summarizes the specifications and performances of the floating buck converters with and without proposed stacked-MOSFETS switch. Firstly, a dramatic increase in both maximum number of driven LEDs and input voltage range can be observed for the floating buck converter with SMS, regardless of the control circuit. The controller supply voltage is the same or lower for converters with stacked switches (Table 1).

Maximum efficiency is higher for the ISMS topologies. Also, when comparing the two ISMS converters, a noticeable efficiency difference, favoring the CrM control method, is evinced. These differences are mainly caused by the variations in average LED current and string voltage drop.

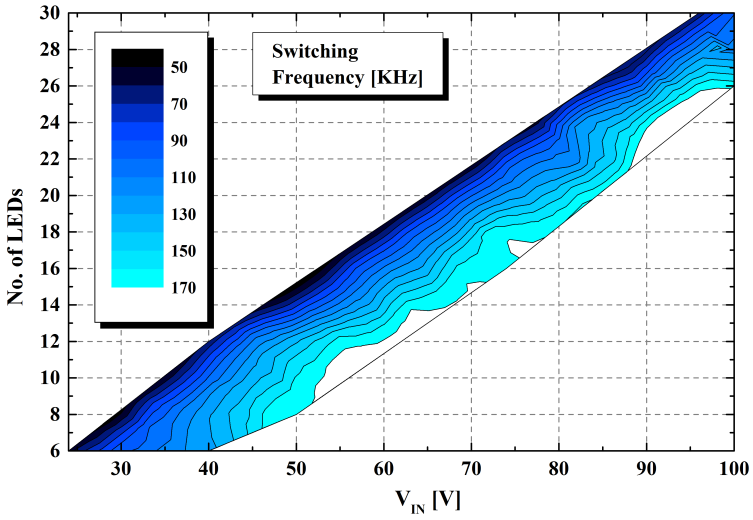

Fig. 12. Measured efficiency results for the ISMS variable OFF time converter.

Table 1. Floating buck converter performances with and without ISMS

Parameter	**Symbol**	**CrM Control**	**CrM Control with SMS**	**Variable OFF time control with SMS**	**Variable OFF time control**
Low Voltage Switch	SW_1	Integrated	Integrated	NTA4001	NTA4001
Power MOSFET	SW_2	–	NDD05N50Z	NDD05N50Z	–
No. of LEDs	n	up to 8	up to 48	up to 30	up to 4
Inductance	L_B	1 mH	1 mH	680 µH	470 µH
Average LED Current	I_{AVG}	250 mA	250 mA	100 mA	100 mA
Controller Supply	V_{SUPPLY}	up to 40 V	12 V	5 V	5 V
Gate Bias Voltage	V_{GG}	–	12 V	7 V	–
Input Voltage	V_{IN}	up to 40 V	up to 240 V	up to 100 V	up to 20 V
Switching Frequency	–	–	25–115 KHz	50–170 KHz	–
Maximum Efficiency	–	94%	97%	93 %	91 %

Another reason for the increased efficiency of ISMS CrM control is the lower switching frequency which incurs smaller switching losses (Table 1). The switching frequency is directly dependent on the inductance value [28]. In consequence, higher efficiencies may be obtained for the variable OFF time control method by changing the inductor.

Table 2 summarizes the main features of the proposed ISMS floating buck converters with CrM (a) and variable OFF time (b) control circuits in comparison with state-of-the-art topologies used in LED driving applications [22], [32], [33], [34], [35]. The performances in terms of output voltage, efficiency and number of series connected LEDs, are comparable or superior for the proposed ISMS converters architectures. Moreover, the ISMS converters deliver similar performances to a commercially available control circuit [35]. The measured LED current and, consequently, the output power are lower for the proposed topologies, but the values were dictated by the application's specific – LED LCD backlighting. Moreover, the user can increase the LED current value by adjusting the R_{FB} resistor.

Table 2. Proposed ISMS converter performances compared to state-of-the-art topologies.

Parameter	**Symbol**	**[22]**	**[32]**	**[33]**	**[34]**	**[35]**	**This Work (a)**	**This Work (b)**
Converter Topology		Single-Stage Flyback Ac/Dc	Single-Stage PFC	Single-Stage buck-boost PFC-flyback	Two-Stage buck-boost/ buck	Floating Buck	Floating Buck	Floating Buck
No. of LEDs	n	3	25	8	60	up to 18	up to 48	up to 30
Output Voltage	V_{OUT}	35 V	150 V	200 V	216 V	–	173 V	96 V
Input Voltage	V_{IN}	AC: 250–520 V	AC: 85–265 V	DC: 200 V	AC: 110 V	DC: up to 65 V	DC: up to 240 V	DC: up to 100 V
LED Current	I_{AVG}	2.1 A	700 mA	500 mA	280 mA	1 A	250 mA	100 mA
Inductance	L_B	–	1.3 mH	3 mH	2 mH	–	1 mH	680 µH
Maximum Efficiency		88.2%	92%	91.7%	93%	96%	97%	93 %

7. Conclusions

This paper proposed a technique to extend the number of driven LEDs in floating buck converters, using an imbalanced stacked MOSFETs switch. The ISMS is comprised of a low power switch with small gate capacitances, and a high voltage power MOSFET biased at a constant gate potential. A Schottky diode was introduced in order to limit the drain-source voltage drop on the low power switch.

An investigation of the ISMS switching sequence was performed. The study

showed that the MOSFET transistors exhibit sequential switching. The main contribution to the total turn-ON/OFF times was given by the power MOSFET. Selecting low gate capacitance transistors, along with a suitable gate bias (V_{GG}), yielded negligible switching sequence durations compared to the total switching period.

A comparative analysis of different control block architectures was carried out. CrM and variable OFF time control circuits emerged as the most suitable for implementing the ISMS technique. Therefore, the MOSFET stack was incorporated in a floating buck converter with both high performing controller architectures. A significant increase in the number of driven LEDs and acceptable input voltages – up to 48 LEDs with 250 V for CrM control and 30 LEDs with 100 V for the variable OFF time architecture – was proven. Also, high efficiencies were obtained for any number of LEDs, for both control methods. Maximum values of 97% and 93% were achieved for the ISMS converter with CrM and variable OFF time control block, respectively. For the latter, the switching frequency was in the 50 kHz – 170 kHz range. Thus, the turn-ON/OFF time measured using variable OFF time control, of up to 350 ns, did not affect proper converter functionality.

Experimental results confirmed that the proposed imbalanced stacked-MOSFETs switch converter exhibits steady operation for high input voltage and large number of series LEDs. Furthermore, the external components' range is not limited by the technique, but rather by the voltage capabilities of the switching transistors chosen for a specific application. The minimal addition of components, effectiveness and ease of implementation recommend the ISMS technique for increasing the number of driven LEDs in any floating buck converter.

References

[1] DisplaySearch Quarterly LED & CCFL Backlight Report, Q4, 2013, [Online], Available 2015: `http://www.displaysearch.com/`

[2] PARK W., PHADKE A., SHAH N., LETSCHERT V., *TV Energy Consumption Trends and Energy-Efficiency Improvement Options*, Ernest Orlando Lawrence Berkeley National Laboratory, July 2011, [Online], Available 2015: `http://eetd.lbl.gov/`

[3] GARCIA J., CALLEJA A. J., COROMINAS E. L., VAQUERO D. G., CAMPA L., *Interleaved Buck Converter for Fast PWM Dimming of High-Brightness LEDs*, IEEE Trans. Power Electronics, Sept. 2011, vol. **26**, no. 9, pp. 2627–2636.

[4] ILIC M., MAKSIMOVIC D., *Interleaved Zero-Current-Transition Buck Converter*, IEEE Trans. On Industry Applications, Nov. 2007, vol. **43**, no. 6, pp. 1619–1627

[5] WINDER S., *Power supplies for LED driving*, Oxford, UK: Newnes, 2008, Chap. 5.

[6] UPRETY S., CHEN H., MA D., *Quasi-Hysteretic Floating Buck LED Driver with Adaptive Off-Time for Accurate Average Current Control in High Brightness Lighting*, Proceedings of the IEEE International Symposium on Circuits and Systems (ISCAS), 2011, pp. 2893–2896, 15–18 May 2011, Rio de Janeiro, Brazil.

[7] KIM H-C, YOON C. S., JEONG D.-K., KIM J., *A Single-Inductor, Multiple-Channel Current-Balancing LED Driver for Display Backlight Applications*, IEEE Trans. On Industry Applications, Nov. 2014, vol. **50**, no. 6, pp. 4077–4081.

[8] EAGAR D., DENICHOLAS J. V., *Current Mode Switcher Having Novel Switch Mode Control Topology And Related Method*, National Semiconductor, U.S. Patent 8 093 826 B1, Jan. 10, 2012.

[9] Datasheet of HV9910B: Universal High Brightness LED Driver, Supertex, [Online], Available 2015: `www.supertex.com`

[10] MEI T., *Buck Constant Average Current Regulation of Light Emitting Diodes*, National Semiconductor, U.S. Patent 8 288 953 B1, Oct. 16, 2012.

[11] IRISSOU P., COLMET-DAAGE E., "Current Sensing for High Voltage Buck Converter", Microsemi, U.S. Patent 8 253 400 B2, Aug. 28, 2012.

[12] MEI T., YANG T., *Circuit and Method for Average-Current Regulation of Light Emitting Diodes*, National Semiconductor, U.S. Patent 7 898 187 B1, Mar. 1, 2011.

[13] Datasheet of LM3407: 350 mA, Constant Current Output Floating Buck Switching Converter for High Power LEDs, Texas Instruments, [Online], Available 2015: `www.ti.com`

[14] SARHAN S., RICHARDSON C., *A Matter of Light – Buck Whenever Possible*, EE Times, May 2008, [Online], Available 2015: `www.eetimes.com`

[15] RUSSELL A. G., BARTHOLOMEUSZ C., *LED Current Bias Control Using A Step Down Regulator*, Catalyst Semiconductor, U.S. Patent 7 323 828 B2, Jan. 29, 2008.

[16] Datasheet of CAT4201: 350 mA High Efficiency Step Down LED Driver, (2011), On Semiconductor, [Online], Available 2015: `http://onsemi.com`

[17] HSIEH C., YANG C., CHEN K., *A Charge-Recycling Buck-Store and Boost-Restore (BSBR) Technique With Dual Outputs for RGB LED Backlight and Flashlight Module*, IEEE Trans. Power Electronics, Aug. 2009, vol. **24**, no. 8, pp. 1914–1925.

[18] ANGHEL V., BARTHOLOMEUSZ C., PRISTAVU G., BREZEANU G., *Variable Off Time Current–Mode Floating Buck Controller – A Different Approach*, Proceedings of the European Solid-State Circuits Conference (ESSCIRC), 2013, pp. 347–350, 16–20 Sept. 2013, Bucharest, Romania.

[19] ANGHEL V., BARTHOLOMEUSZ C., VASILICA A., PRISTAVU G., BREZEANU G., *Variable Off Time Control Loop For Current–Mode Floating Buck Converters in LED Driving Applications*, IEEE J. Solid-State Circuits, July 2014, vol. **49**, no. 7, pp. 1571–1579.

[20] MENTZE E. J., HESS H., BUCK K. M., WINDLEY T. G., *A Scalable High-Voltage Output Driver for Low-Voltage CMOS Technologies*, Very Large Scale Integration (VLSI) Systems, IEEE Transactions on, vol. **14**, no. 12, pp. 1347–1353, Dec. 2006.

[21] PAGE S., WAJDA A., HESS H., *High Voltage Tolerant Stacked MOSFET In A Buck Converter Application*, Microelectronics and Electron Devices (WMED), 2012 IEEE Workshop on, pp. 1–4, 20 Apr. 2012.

[22] WANG L., WU X., PENG F. Z., *High Input Voltage Single-Stage Flyback AC/DC LED Driver Using Series-Connected MOSFETs*, Applied Power Electronics Conference and Exposition (APEC), pp. 2379–2384, Feb 2012.

[23] BUONOMO S., MUSUMECI S., PAGANO R., PORTO C., RACITI A., SCOLLO R., *Driving a New Monolithic Cascode Device in a DC-DC Converter Application*, IEEE Transactions on Industrial Electronics, vol. **5**, no. 6, pp. 2439–2449, June 2008.

[24] GRBOVICÌ P.J., *High-Voltage Auxiliary Power Supply Using Series-Connected MOSFETs and Floating Self-Driving Technique*, IEEE Transactions on Industrial Electronics, vol. **56**, no. 5, pp. 1446–1455, January 2009.

[25] MANIKTALA S., *Switching Power Supplies A to Z*, Oxford, UK: Newnes, 2006, Chap. 5.

[26] KAZIMIERCZUK M. K., *Pulse–width modulated DC–DC power converters*, Hoboken, NJ, US: John Wiley & Sons, 2008, Chap. 13.

[27] WU X., YANG J., ZHANG J., QIAN Z., *Variable On-Time VOT Controlled Critical Conduction Mode Buck PFC Converter for High-Input ACDC HB-LED Lighting Applications*, IEEE Trans. Power Electronics, Nov. 2012, vol. **27**, no. 11, pp. 4530–4539.

[28] BASSO C., *Switch–mode power supplies*, New York, NY, US: McGraw–Hill, 2008, Chap. 1 and 2.

[29] Datasheet of FL7701: Smart LED Lamp driver with PFC Function, Fairchild Semiconductor, [Online], Available 2015: `www.fairchildsemi.com`

[30] Datasheet of NDD05N50Z: Power MOSFET 500 V 4.7 A 1.5 Ohm Single N-Channel, (2013), On Semiconductor [Online], Available 2014: `http://onsemi.com/`

[31] Datasheet of NTA4001N: Small Signal MOSFET 20 V 238 mA 1.5 Ohm Single N-Channel SC-75 with ESD Protection, (2011), On Semiconductor [Online], Available 2015: `http://onsemi.com`

[32] QIU Y., WANG H., HU Z., WANG L., LIU Y. F., SEN P. C., *Electrolytic-Capacitor-Less High-Power LED Driver*, Energy Conversion Congress and Exposition (ECCE), pp. 3612–3619, September 2014.

[33] CHENG C.-A., YANG F.-L., KU C.-W., YEN C.-H., *A Novel Single-Stage High Power LEDs Driver*, International Conference on Power Electronics and ECCE Asia (ICPE & ECCE), pp. 2733–2740, 2011, Jeju, South Korea.

[34] CHENG H.-L., LIN C.-W., *Design and Implementation of a High-Power-Factor LED-Driver With Zero-Voltage Switching-On Characteristics*, IEEE Transactions on Power Electronics, vol. **29**, no. 9, pp. 4949–4958, Sept 2014.

[35] Datasheet of LM3414HV: [34] 1A 60W Common Anode Capable Constant Current Buck LED Driver Requires No External Current Sensing Resistor, (2013), Texas Instruments, [Online], Available 2015: `www.ti.com`